Iris Characteristics Affecting Far Peripheral Vision and Negative Dysphotopsia

Michael J. Simpson, Ph.D.

Simpson Optics LLC, Arlington, TX 76012, USA

Maria Muzyka-Wozniak, M.D., Ph.D.

Spektrum Eye Clinic, Wroclaw, Poland

Corresponding author:

Michael J. Simpson, Ph.D.

Simpson Optics LLC,

3004 Waterway Ct, Arlington, TX 76012

USA.

Iris Characteristics Affecting Far Peripheral Vision and Negative Dysphotopsia

Purpose: To evaluate how the iris obstructs rays at large visual angles.

Setting: Consultancy and Eye Clinic

Design: Experimental study.

Methods: Anterior segment optical coherence tomography (OCT) images were exported from Visante for 21 normal, 20 short, and 19 long eyes evaluated previously, and 3 eyes with negative dysphotopsia reports. Iris characteristics were manually identified, including the maximum iris thickness and its distance from the pupil, and the gap between the iris and IOL. Zemax raytrace software was used for optical modeling.

Results: Preop and postop iris dimensions were similar, with a mean maximum thickness of 0.47 ± 0.08 mm at 0.94 ± 0.19 mm radially from the pupillary margin. The mean pupillary plane distance from the corneal epithelium moved from 3.23 ± 0.50 mm preop to 3.99 ± 0.26 mm postop, and the mean gap between the posterior iris and the IOL was 0.50 ± 0.24 mm, with a systematic increase with axial length for both parameters. The anterior iris surface obstructed light at very large angles, and contributed to the limiting visual angle for rays focused by the IOL (though light from lower angles also bypassed the IOL). Models for the eyes with negative dysphotopsia reports had dark retinal regions between the focused image and peripheral light for small pupils.

Conclusions

Rays at very large angles can be obstructed by the anterior iris surface, which can be modeled to have a triangular profile near the pupillary margin. This limits the visual field for light focused by the IOL.

Iris Characteristics Affecting Far Peripheral Vision and Negative Dysphotopsia

Recent theoretical evaluations exploring the cause of negative dysphotopsia with intraocular lenses (IOLs) have found that there is limited information about peripheral light rays entering the eye [1–3]. At very large visual angles, light enters the eye from the side, rather than from the front, and for light to be visible, it needs to first pass through a clear region of the cornea, and then also avoid obstruction by any part of the iris. There do not appear to be any publications that document the limiting parameters of the cornea and the iris for these peripheral rays. The rays at large angles are all from the temporal direction, because nasal visual field angles are limited to much lower values by the cheek, nose, and eyebrow, and there have been no reports of negative dysphotopsia in the nasal visual field.

This paper primarily addresses questions about the iris rather than the cornea, and there has recently been increased measurement of the anterior segment, since opening the anterior chamber (AC) angle after cataract surgery may lower the intraocular pressure (IOP) and reduce the risk of glaucomatous damage, particularly in short eyes with primarily narrow AC angles [4–7]. This has led to many publications that have images of the anterior segment, with various measured parameters that describe changes in the angle, but these rarely include the data about the iris that are useful for evaluating light rays at large angles. Occasionally the distance between the posterior iris and the IOL has been reported [8], and often the iris diameter, and information about the angle are given, but there has been limited information about the iris thickness, or the iris location with respect to the IOL. This may be partly due to the fact that the iris is so variable that it is difficult to characterize, and that has been addressed in this paper.

Schematic model eyes have been used for many years to evaluate optical properties [9–11], but these were typically created primarily to evaluate foveal vision, and if the model includes an iris, it is typically only a thin surface. Most models were originally developed for the phakic eye, and some include methods for simulating the gradient index crystalline lens [10]. Wide-field eye models have also been described, but

these do not include detailed corneal or iris information [12], and are typically used only up to modest visual angles (e.g. 40 [0]), though some are used as a method for scaling the peripheral retina [13]. The pseudophakic eye is much simpler than the phakic eye because an IOL has a single refractive index. Both paraxial and more realistic model eyes are used routinely in cataract surgery to estimate the IOL power that is required for an individual eye, but these are typically only used on-axis. The corneal surfaces used in model eyes typically use a conic constant to create central asphericity, but it is not clear whether the accuracy of the models has ever been verified out to the edge of the clear corneal region. Simplified eye models are used here, with a new model for the central thick iris region, as an initial exploration of the effects that this has on peripheral imaging.

This paper is based on earlier work evaluating changes to the anterior chamber depth and iris following cataract surgery [14]. Many of the same images are used, but they were exported from the measurement equipment, and evaluated separately to estimate various parameters that describe the iris. Raytrace software was then also used to estimate characteristics for the limiting visual angle for light imaged by an IOL. Additional images for three eyes of 2 patients who perceive negative dysphotopsia were also included and evaluated.

Patients and Methods

Anterior segment optical coherence tomography (AS OCT) (Visante, Carl Zeiss Meditec AG) preoperative and postoperative images that had been evaluated previously were exported from Visante for 21 normal, 20 short and 19 long eyes [14]. Figure 1 gives an example of a postoperative image, and the length of the scale bar in each image was used to calibrate the image size. Additional images for 3 eyes of 2 patients who perceived peripheral dark shadows were also used. ImageJ software was used to manually identify the coordinates of features on the images, and Matlab was used to calculate distances.

The iris profile cross-section is a complicated structure, and it has characteristics that vary considerably from eye to eye (Figure 2). After reviewing the images, one feature that seemed to be present for most of the eyes was a region of maximum thickness relatively close to the iris margin. This would be the location that might obstruct peripheral rays the most, and two points were identified by hand to characterize it, with an estimate for both the most anterior point, and the corresponding point on the posterior iris in the axial direction (Figure 1). The iris profile close to the optical axis was quite variable, and although the iris in Figure 1 is representative of a typical shape, the surface might curve outwards or inwards for different eyes. It was found that the fundamental shape that might obstruct light could be characterized by the 4 additional points indicated in Figure 1. One point is used to define the pupil diameter itself, at the iris margin on the anterior surface. The profile in this region was rarely a distinct apex, however, and an additional point was used to define the posterior iris surface near the iris margin, even though the points are typically very close. The other two points were manually chosen to characterize the local profile, and they were typically the points with maximum deviation from a straight line on the anterior and posterior surfaces. The smallest distance between the posterior iris surface and the anterior IOL surface was also recorded. Values of thicknesses and distances were estimated for the iris on both the nasal and temporal sides, and they were averaged together. The measurements were all made by a single observer (MJS).

The Zemax raytrace software was used to model individually many of the primary characteristics of the pseudophakic eyes, and to estimate limiting visual angles for peripheral light rays. The corneal power and axial length values were available for each eye from IOLMaster, and these were used to specify the anterior corneal radius (=337.5/(corneal power)) and axial length. The posterior corneal radius of curvature is not normally measured, and a value was estimated from the anterior surface using a typical radius ratio of 0.84 times the anterior radius [12]. An attempt was made to estimate conic constant values for each eye using points taken from the images, but it was not clear how accurate these were from the

OCT images, and ultimately they were not used in the models. Published conic constant values for the cornea do not usually specify the diameter of the region for which they are expected to be accurate, and they have typically been created to describe the optical quality of the central corneal region only. Standard conic constant values were used instead for all eyes for this initial evaluation of limiting visual angles, with -0.26 for the anterior surface, and -0.24 for the posterior surface [2].

The iris was modeled using two-surfaces, with the individual diameter and thickness parameters for each eye as the average of the values for the two sides in the images. The pupil was set at the axial location of the inner points on the anterior iris surface, and an additional opaque aperture was added 0.5 mm in front of it, with a diameter that was 1.8 mm larger. This essentially models the central region of the iris as a simple triangle, which captures the predominant properties of the central region, and how the light rays are affected. The IOL power for emmetropia was estimated using axial raytracing for each eye, by placing the IOL at the correct axial location, and adjusting the IOL power until the axial image was in focus. The model eyes were all centered on the optical axis, and 5 degrees was added to input ray angles to estimate the visual angle. The OCT images did often include information about the angle between the visual axis and the optical axis, and the centration of the iris, but it was rarely possible to evaluate the IOL centration and tilt, and the simpler model was used for consistency. A 3 mm diameter pupil was used for all the calculations.

The rays that were evaluated using the models were (i) the maximum input angle for a ray that can pass through the IOL, and (ii) the minimum input angle where a ray just misses the IOL The maximum ray angle is an upper limit for focused rays, though the actual ray image location can also be affected by aberrations [2]. The first ray missing the IOL is at an angle that is closer to the start of the "vignetting" that happens at the lens for light at large angles [1,2], which is where the main focused image starts to dim.

These two limiting angles together characterize a potential for "dark shadows", and they are uniquely defined.

In addition to the pseudophakic eye images, the earlier phakic eye images were also evaluated using similar methods. The lens location, and the iris characteristics, were evaluated and compared to those of the same pseudophakic eye. Preoperative and postoperative images were also superimposed with widely-used software (Microsoft Powerpoint), where one image was set as a rectangle object with a semitransparent "picture fill", and visually adjusted to match the other image. Distracting overlays were obscured by copying adjacent regions using Microsoft Paint.

Results

As a person ages over many decades, the natural crystalline lens thickens, and it pushes the iris forward in the anterior chamber. The iris is always in contact with the crystalline lens, and all the light that enters the pupil enters the lens. When the natural lens is removed, however, the iris moves to the posterior, and there is usually a gap between the posterior iris surface and the IOL. The IOL is also much smaller than the natural crystalline lens, with a single refractive index rather than a gradient index, and the overall optical effects at large angles are different to those of the phakic eye. Light rays entering the pupil at large angles might now pass through the gap instead of the lens. The posterior movement of the iris also opens up the AC angle, which is beneficial for eyes with narrow angles or primary angle closure glaucoma.

Some of the main differences between preoperative and postoperative eyes are illustrated in Figure 3 where images have been superimposed. These are representative eyes that show different levels of posterior iris movement following surgery, where Fig 3(b) is for a typical eye, Fig 3(a) is for an eye with a

very large change, and Figure 3(c) is for an eye where the iris plane does not seem to move at all (though this was also for a younger eye). The posterior crystalline lens surface is not visible in the OCT images, but the crystalline lens has been sketched, using a published equation for the average thickness that uses the age of the patient [15]. The IOL surfaces are also sketched, though they are only approximate.

The main data characterizing the iris are plotted in Figure 4. Figure 4(a) plots the maximum iris thickness against the distance from the pupillary margin for both preoperative and postoperative eyes. The values fall within modest ranges, with a mean maximum thickness of 0.47 ± 0.08 mm at 0.94 ± 0.19 mm from the pupil margin. Figure 4(b) shows that the values did not vary systematically with pupil diameter, and they cover a normal range of pupil diameters (range 2.5-3.7mm, mean 3.18±0.35 mm, for postop eyes). The pupil diameters were effectively set by the standard photopic room illumination of 120-150 lux, which corresponds to a luminance level needed for most daily activities except reading and table work. There are no data that cover a range of illumination levels for the same eye. Fig 5 compares the preoperative and postoperative iris values more directly, using just the distance parameter. No adjustment was made for the tilting of the iris, which was particularly prominent for some preoperative eyes, but the plot shows that the values are very similar, even so.

The iris moves posteriorly following cataract surgery, and the iris depth (the distance from the anterior cornea to the effective pupil location) is plotted in Fig 6(a) against the axial length. This plot indicates that shorter eyes have the iris closest to the cornea preoperatively, but it also shows that those eyes have the greatest movement of the iris to the posterior following surgery. The average gap between the iris and the IOL also increase with axial length, and this is plotted in Fig 6(b). Something that was unexpected was that two of the short eyes had an extremely small gap between the posterior iris and the IOL on at least one side, and two others had no gap at all. These eyes were not included in the modeling of limiting angles.

A review of the data and the postop images found that for optical modeling a triangle could be used as a first approximation to the iris region close to the pupillary margin. The posterior surface is often flat or gently curved, and although there is usually a difference between where rays at large angles might be occluded by either the anterior iris or the posterior iris, which would be for rays hitting different sides, these points are relatively close. The iris was implemented in Zemax as two opaque apertures (Fig 7), where the anterior one is 0.5 mm in front of the other, with a radial opening that is 0.9 mm larger. This effectively creates a wedge-shaped region near the iris margin. Limiting rays are illustrated in Fig 7, where the last ray focused by the IOL grazes the anterior iris surface (blue ray), and the first ray missing the IOL grazes the posterior inner iris (red ray).

The results from limiting ray calculations are plotted in Figure 8 against axial length, where the limiting rays were calculated for each eye using its own pupil diameter. This uses the simplified individualized eyes described in the methods section, where there are no pupil or lens decentrations, and all eyes have the same corneal asphericity. The optical input angles used for the raytrace were converted to visual angles by adding 5 degrees. The average maximum focused ray visual angle was approximately 95 degrees for the normal eyes, and the average visual angle for the first ray to miss the IOL was 83 degrees. The pupil diameter strongly affects the latter value.

The raytrace eye models were also used to estimate the clear corneal diameter on the anterior surface that was needed for the limiting focused ray postop, and these are plotted in Figure 9. The white-to-white values were not recorded for these eyes, but these values generally fall within a typical range, with a mean value of about 12 mm diameter. The OCT images sometimes have a V-shaped characteristic at the corneal limbus, and this can be seen in Fig 1 and Fig 3(b), but it is not clear simply from the image how this corresponds to the anatomical corneal limbus. This feature was not available consistently, and it was not compared to the values estimated for the required clear cornea.

The 3 eyes where dark shadows were seen in this series of patients were all short eyes with IOL powers of over 30D. Their iris characteristics and limiting angles are included in the values given earlier, but an evaluation of negative dysphotopsia really requires a comparison of where the limiting rays hit the retina [2]. Model eyes were set up in Zemax for these two patients, and superimposed raytrace plots are given in Figure 10 for the left eye of both, reoriented as though for a right eye viewed from above. The pupil diameter is 2.5mm in each case, and the blue rays depict the last focused ray, with the red ray depicting the first ray that misses the IOL. In both cases, there is a gap between the limit of the focused image, and the start of illumination from light missing the lens, which may be the region reported as a dark shadow by a patient. Both eyes of patient 1 saw peripheral dark shadows, with the eyes being broadly similar, and with typical iris parameters, though the eyes had a 3.7 mm diameter pupil in the OCT images. The OCT image for patient 2 actually had a 2.5 mm diameter pupil.

Discussion

The pupil of the eye is typically depicted as a thin structure for optical raytrace modeling, but for light entering the eye at very large visual angles, the anterior iris surface can act as a limiting aperture. A simple theoretical model for the complex shape of the central iris has been created here using the thickness and radial location of the first thick iris region, when moving outward from the pupillary margin. This leads to a simple triangular approximation for the inner iris profile, which can be used in raytrace software to evaluate the optical properties of the eye at large angles. Using rounded numbers, the iris is approximately 0.5 mm thick at 1 mm from the pupil edge.

One limitation of the pupil diameters in this study is that they were set naturally by the illumination level of the OCT system, though they cover a typical range for the older eye under normal illumination levels. The characterization of the inner iris cross-section described here was developed from an observation of the OCT images, rather than from an evaluation of the anatomy, but it is possible that the

dimensions are related to the sphincter muscle, and to the collarette. The work reported in an extensive study of the pupil by Loewenfeld [16] discusses the sphincter muscle, and that its radial width changes with pupil diameter. Unfortunately, this work predates the introduction of OCT instruments, and it does not appear to include any information about iris thickness, though an extensive bibliography is included. The main discussion is really about pupil diameter changes, though there are comments about the "pigment ruff", or "iris ruff", where the posterior pigment epithelium of the iris can wrap around from the posterior iris surface into the pupil opening. Illustrations from Hogan et al are used to describe this [17], and comments are made that the pupil opening that is visible in color images is typically larger than the actual pupil opening, but that the correct effective pupil can be recorded with infrared illumination. This is because the pigment ruff is not normally visible when it is viewed against a dark pupil opening. From this description, it is possible that the pigment epithelium may correspond to the bright layer that is visible in the OCT images on the posterior of the iris, which often intrudes into the pupil. This surface was used to characterize the iris when recording the full dataset of points, but it was not included in the simplified 2-surface model for the iris, which uses the main pupil plane for the posterior surface.

The iris cross section is generally much more complicated than the structure modeled using 2 planar surfaces, but the identification of the main thick region captures the fundamental properties. The use of 6 points to characterize the more central iris structure captures a great deal of the shape of the iris that affects oblique light transmission, and points like these could be routinely monitored in OCT images. The points could also be chosen and evaluated in a more sophisticated manner. The iris is typically pushed forward in the older eye, which gives it additional curvature. This seems to be partially reduced as the iris moves to the posterior in the postop eye, though a residual curvature is often visible in the images. This effect was not evaluated. The measurements in this paper were made by a single investigator, but any bias due to this is likely to be very small, and to be overwhelmed by the variety of the characteristics for the different eyes. The overall methods have the various inherent limitations described above,

particularly those due to eye rotation and iris curvature, the identification of specific points on the iris, and the use of a single image for each eye. There do not appear to be any previous data about the physical tapering characteristics of the iris near the iris margin, and there were no expectations as to what the results might be, which might have led to bias. This paper can be thought of as an initial study of these parameters. The gap between the iris and the IOL is about 0.5 mm for an eye with an average axial length, which is similar to values reported elsewhere [8], but there can be a lot of variation in this value. This provides an opportunity for light to illuminate the retina directly at large angles, without passing through the IOL. The centration and tilt of the IOL can affect the amount of this illumination that is possible with small pupils, as can the centration of the iris itself. The pupil diameter has the greatest effect on this type of illumination, however. The iris moved to the posterior following cataract surgery by about 0.8 mm for an average axial length, but there was greater movement for shorter axial lengths.

The average human eye is thought to see out to a visual angle of 105 degrees, but it is not clear if the actual limit has ever been determined for large patient populations [3]. The maximum visual angle may be affected by the limit of the sensitive retina, which has no measurement method, in addition to the other parameters discussed here, which are the iris and clear cornea. The limiting visual angle values for the focused image calculated here are all less than 100 degrees, but this is approximately the angle at which absolutely no light passes through the IOL at all for the eyes that are modeled. A rough approximation for the mean visual angle at which the main image focused by the IOL becomes significantly dim might be to take the mean value for the angles at which the 1st ray misses the IOL, and the last ray is focused by the IOL, which is about 88 degrees for the calculations for the normal eye. The light that bypasses the IOL also provides illumination, primarily from lower visual angles, with the "apparent" image locations not corresponding to those of the focused image.

The limiting ray evaluation indicates that a clear corneal diameter of 11.5 – 13 mm is needed in order for the cornea not to be the limiting aperture, which is in agreement with the typical white-to-white value

recorded for the eye. This value can vary from eye to eye, however, and it can be affected by other parameters such as the IOL decentration and tilt, the pupil decentration, and the limit of the sensitive retina. The effects of these variations were not evaluated.

Two of the subjects in this study perceived negative dysphotopsia for longer than 6 months after surgery, and the raytrace modeling indicated that for small pupils there would be a gap between the limit of the main image, and the start of peripheral retinal illumination by light that missed the IOL completely. This is likely to be the cause of the shadow reports, but this has not been confirmed clinically. However, these patients had high hyperopic refractive errors preoperatively, and found the effect tolerable. Patients who are particularly bothered by negative dysphotopsia are thought to have refractive characteristics that are typically closer to those of an average eye[18].

The improvements described here in modelling the iris more exactly may lead to a better understanding of the optics of the pseudophakic eye, particularly with respect to negative dysphotopsia. Clinical evaluations of negative dysphotopsia have sometimes included values for the gap between the iris and the IOL, but they have never included the effects of iris thickness and corneal clarity on peripheral light rays, or detailed evaluations of light interactions with the peripheral regions of actual fabricated IOLs, which may vary by lens style. The various figures may also be of interest for other aspects of cataract surgery planning, such as the plots in Figure 7, where changes in iris location between preoperative and postoperative eyes, and the physical space between the iris and the IOL, are shown to vary strongly with axial length

What was known

- The iris is normally modeled for optical raytracing as a thin structure, and the distance between the iris and an intraocular lens is rarely measured.

What this paper adds

- The iris surrounding the pupil can be modeled using a triangular cross-section, and the anterior iris surface obstructs rays at very large angles.

- The distance between the iris and the IOL varies with axial length

References

1.   Simpson MJ. Vignetting and negative dysphotopsia with intraocular lenses in " far peripheral
      vision ." *J Opt Soc Am A*. 2015;32(9):1672-1677. doi:10.1364/JOSAA.32.001672.

2.   Holladay JT, Simpson MJ. Negative dysphotopsia: Causes and rationale for prevention and
      treatment. *J Cataract Refract Surg*. 2017;43(2):263-275.

3.   Simpson MJ. Mini-review: Far peripheral vision. *Vision Res*. 2017;140C:96-105.

4.   Hayashi K, Hayashi H, Nakao F, Hayashi F. Changes in anterior chamber angle width and depth
      after intraocular lens implantation in eyes with glaucoma. *Ophthalmology*. 2000;107(4):698-703.

5.   Jacobi P, Dietlein T, Lüke C, Engels B, Krieglstein G. Primary phacoemulsification and intraocular
      lens implantation for acute angle-closure glaucoma. *Ophthalmology*. 2002;109(9):1597-1603.

6.   Hata H, Yamane S, Hata S, Shiota H. Preliminary outcomes of primary phacoemulsification plus
      intraocular lens implantation for primary angle-closure glaucoma. *J Med Invest*. 2008;55(3-
      4):287-291.

7.   Dooley I, Charalampidou S, Malik A, Loughman J, Molloy L, Beatty S. Changes in intraocular
      pressure and anterior segment morphometry after uneventful phacoemulsification cataract
      surgery. *Eye (Lond)*. 2010;24(4):519-526.

8.   Pereira FAS, Cronemberger S. Ultrasound biomicroscopic study of anterior segment changes after
      phacoemulsification and foldable intraocular lens implantation. *Ophthalmology*.
      2003;110(9):1799-1806. doi:10.1016/S0161-6420(03)00623-7.

9.   Atchison DA, Smith G. *Optics of the Human Eye*. Edinburgh: Butterworth-Heinemann; 2002.

10.   Liou HL, Brennan N a. Anatomically accurate, finite model eye for optical modeling. *J Opt Soc Am*

A Opt Image Sci Vis. 1997;14(8):1684-1695. http://www.ncbi.nlm.nih.gov/pubmed/9248060.

11.   Navarro R. Adaptive model of the aging emmetropic eye and its changes with accommodation. *J Vis*. 2014;14:1-17. doi:10.1167/14.13.21.doi.

12.   Goncharov A V, Dainty C. Wide-field schematic eye models with gradient-index lens. *J Opt Soc Am A Opt Image Sci Vis*. 2007;24(8):2157-2174. http://www.ncbi.nlm.nih.gov/pubmed/17621320.

13.   Suheimat M, Zhu H, Lambert A, Atchison DA. Relationship between retinal distance and object field angles for finite schematic eyes. *Ophthalmic Physiol Opt*. 2016;36(4):404-410. doi:10.1111/opo.12284.

14.   Muzyka-Wozniak M, Ogar A. Anterior chamber depth and iris and lens position before and after phacoemulsification in eyes with a short or long axial length. *J Cataract Refract Surg*. 2015;42:563-568. doi:10.1016/j.jcrs.2015.12.050.

15.   Atchison DA, Markwell EL, Pope JM, Swann PG. Age-related changes in optical and biometric characteristics of emmetropic eyes. *J Vis*. 2008;8(4):29, 1-20. doi:10.1167/8.4.29.Introduction.

16.   Loewenfeld IE. *The Pupil: Anatomy, Physiology, and Clinical Applications*. Boston MA: Butterworth; 1999.

17.   Hogan MJ, Alvorado JA, Wedell JE. *Histology of the Human Eye*. Philadelphia: W. B. Saunders; 1971.

18.   Henderson BA, Geneva II. Negative dysphotopsia: A perfect storm. *J Cataract Refract Surg*. 2015;41(10):2291-2312. doi:10.1016/j.jcrs.2015.09.002.

Figure Captions

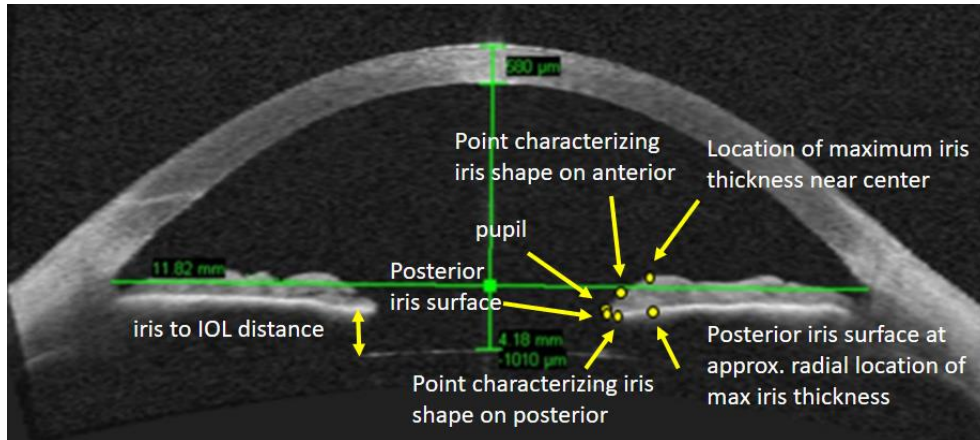Figure 1. Example OCT image with iris points identified.

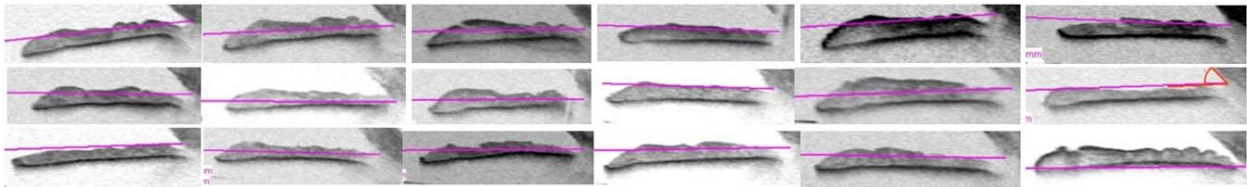Figure 2. Example iris profiles displayed as negatives. The pink line is the scale line.

Figure 3. Superposition of preoperative and postoperative images for representative eyes with different levels of iris movement, with yellow lines sketching the preoperative lens surfaces, and green lines sketching postoperative lens surfaces. The mean corneal power, axial length, approximate IOL power, and age are listed for each eye. (a) K=45.6 D, L=21.90 mm, IOL = 25.5 D, Age= 70. (b) K= 43.4 D, L=23.04 mm, IOL=23.5 D, Ag= 81. (c) K= 40.8 D, L=21.51 mm, IOL=33 D, Age=46 (the iris plane does not change, and the smaller pupil is preoperative).

Figure 4. (a) Thickness of thickest iris region vs distance from pupillary edge. (b) Thickness of thickest iris region vs pupil diameter
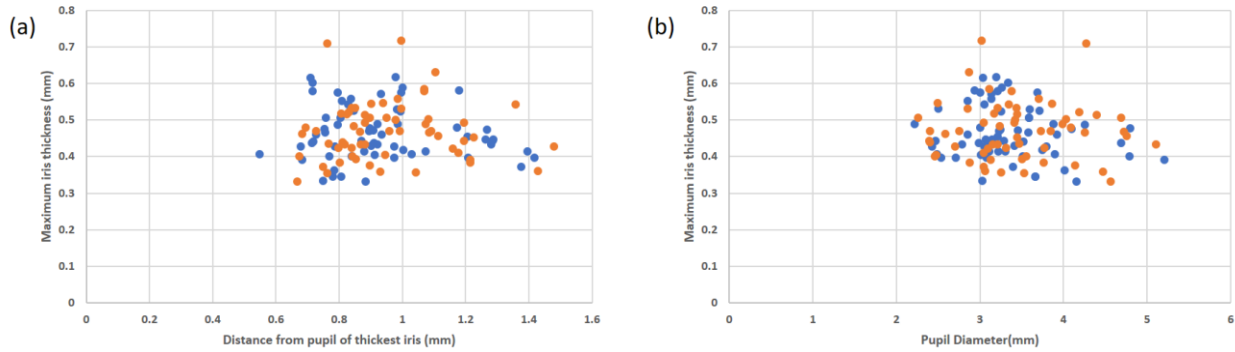

Figure 5. Comparison of distance of thickest iris region from pupillary edge: postoperative vs preoperative.
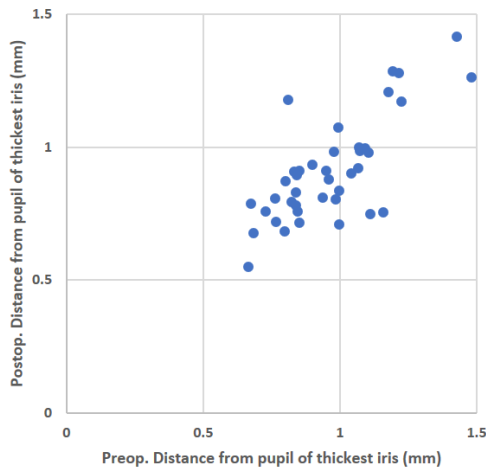

Figure 6. (a) Axial distance from anterior cornea to effective pupil vs axial length (orange preoperative; blue postoperative). (b) Mean gap between posterior iris and anterior IOL vs axial length
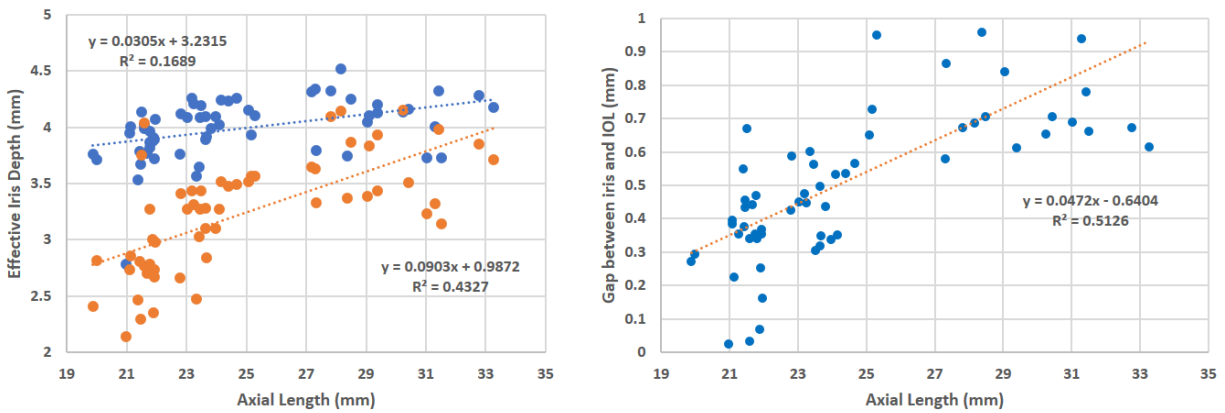
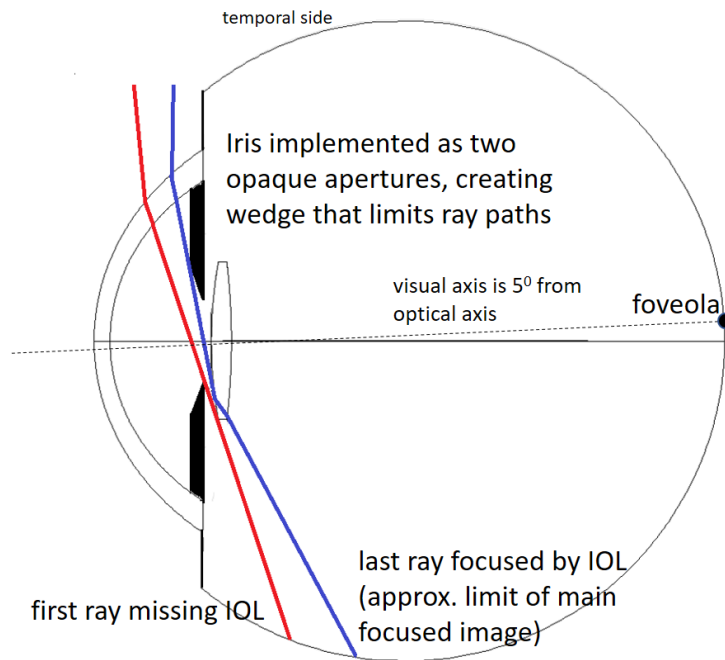Figure 7. Optical model used for raytracing showing limiting rays.

temporal side

Iris implemented as two
opaque apertures, creating
wedge that limits ray paths

visual axis is 5^0 from
optical axis

foveola

last ray focused by IOL
(approx. limit of main
focused image)

first ray missing IOL

Figure 8. Estimation of limiting ray angles for each eye.

Max. visual angle for ray through IOL

Visual angle for first ray missing IOL

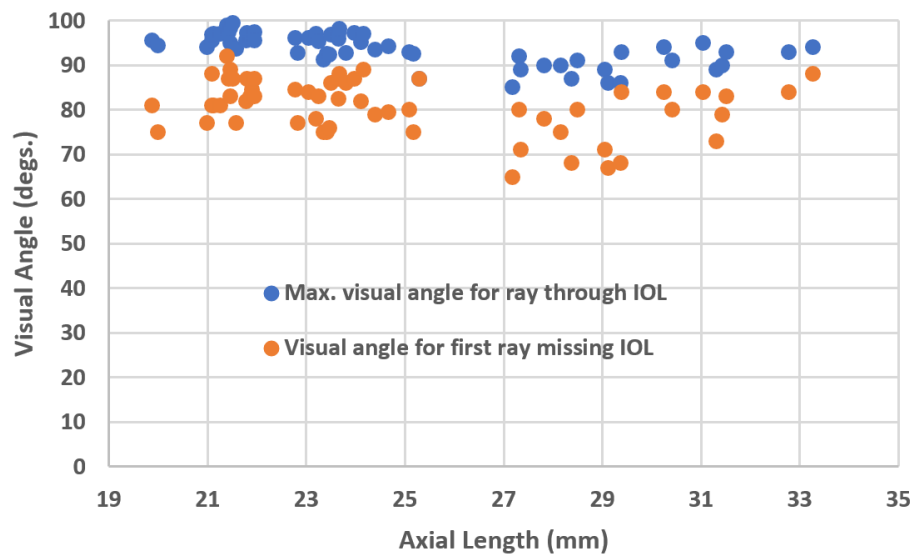Visual Angle (degs.)

Axial Length (mm)

Figure 9. Estimated clear corneal diameter needed for the limiting postop focused ray.
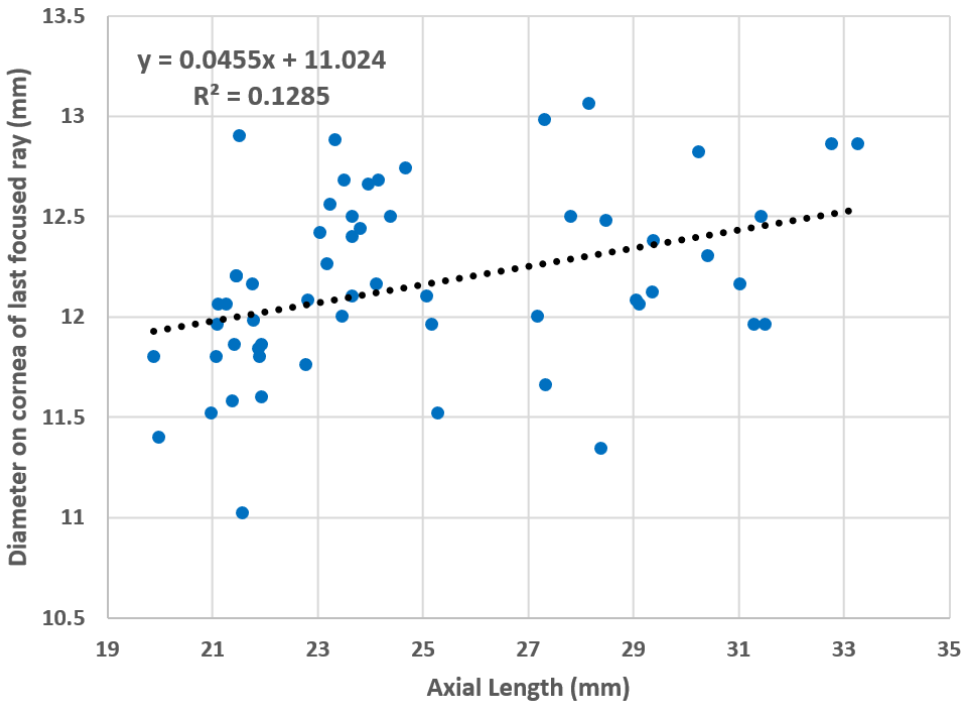

Figure 10. Raytrace plots from Zemax showing the last ray focused by the IOL (blue) and the first ray missing the IOL (red) for a 2.5 mm diameter pupil. The input visual angles do not necessarily correspond to equivalent retinal regions used by the phakic eyes. (a) Patient 1. Last focus 96 degrees. 1st miss 82 degrees. (b) Patient 2. Last focus 90 degrees. 1st miss 81 degrees.